

Liquid hyperpolarized ^{129}Xe produced by phase exchange in a convection cell

T. Su, G. L. Samuelson, S. W. Morgan, G. Laicher, and B. Saam
Department of Physics, University of Utah, Salt Lake City, Utah 84112

(Received 13 May 2004; accepted 26 July 2004)

We present a method for the production of liquid hyperpolarized ^{129}Xe that employs spin-exchange optical pumping in the gas phase and subsequent phase exchange with a column of xenon liquid. A convection loop inside the sealed glass cell allows efficient transfer of magnetization between the gas and liquid phases. By condensing to liquid a large fraction of the sample, this scheme permits the polarization of many more ^{129}Xe atoms in a given sealed-cell volume than would otherwise be possible. We have thus far produced a steady-state polarization of 8% in 0.1 mL of liquid with a characteristic rise time of ≈ 15 min. © 2004 American Institute of Physics.

[DOI: 10.1063/1.1793350]

Nuclear spin polarizations on the order of 0.1 can be generated in ^{129}Xe gas by spin-exchange optical pumping (SEOP).¹ The enormous sensitivity enhancement for nuclear magnetic resonance (NMR) realized with these hyperpolarized gases has led to many and varied applications,^{2–4} and to an intense interest in optimizing production methods.^{5–7} NMR and magnetic resonance imaging (MRI) have recently been used to study convection near the Xe gas-liquid interface.^{8,9} In those experiments, hyperpolarized ^{129}Xe was produced entirely in the gas phase and then condensed to liquid. By contrast, we show here that spin exchange and phase exchange in an appropriately designed gas-convection cell can generate steady-state liquid ^{129}Xe polarizations of 5–10% in ≈ 15 min. If all xenon in these cells were in the gas phase, the high xenon density would preclude efficient SEOP due to the strong Rb-Xe spin-rotation interaction¹⁰ that rapidly relaxes the Rb electron spin.

The key innovation in this work is the xenon convection cell shown in Fig. 1. The permanently sealed cells are made of Corning 7740 (Pyrex) glass and are coated with SurfaSil¹¹ to inhibit ^{129}Xe wall relaxation.^{12,13} The xenon gas is enriched to 86% ^{129}Xe .¹⁴ Specific contents for each cell are given in Table I. Laser light enters the 8 cm³ spherical chamber horizontally from the right. A U-shaped 6-mm-i.d. tube extends from the sphere towards the rear of the cell, and a small reservoir (0.2 cm³) for the liquid is located at the bottom rear of the cell. One NMR coil is wound around the reservoir to monitor the liquid polarization; an additional coil is positioned around the upper arm to detect the gas-phase signal. The two-chambered oven/refrigerator (not shown) is constructed from high-density polyethylene with a glass window in front to pass the laser light. Air forced through a filament heater is used to heat the front chamber to between 360–380 K. Gas boiled off from a liquid-nitrogen dewar is used to cool the rear chamber to 160–165 K. Separate temperature sensors allow for feedback and temperature control in both chambers. The apparatus was placed in a horizontal-bore superconducting solenoid with a field of 0.94 T. NMR studies were conducted with an Apollo NMR spectrometer¹⁵ running at the ^{129}Xe Larmor frequency of 11.1 MHz. SEOP was performed with circularly polarized 795 nm light from a frequency-narrowed¹⁶ 15 W diode-laser array directed along the magnet bore.

With the laser blocked, an unpolarized cell was loaded and allowed to come to phase equilibrium with the front of the oven/refrigerator held at 373 K and the back held at 163 K. The Xe vapor pressure inside the cell is about 900 mbar at 163 K. The remaining Xe atoms in the cell condensed as liquid in the reservoir.¹⁷ NMR signal intensities were recorded by measuring both the initial height of the free-induction decay and the area under the Fourier-transformed spectrum. After recording the thermal-equilibrium liquid signal, the laser was unblocked for 30–60 min, allowing the gas and liquid signals to reach their steady-state values. The liquid polarization was then assessed by comparing the hyperpolarized and thermal-equilibrium signal intensities.¹⁸ In one case with the 6520 mbar cell, we used the NMR coil surrounding the liquid reservoir to estimate the gas polarization by inverting the entire apparatus, allowing gas to fill the reservoir volume. The gas polarization was then estimated based on a comparison of the gas-phase signal with the thermal-equilibrium liquid signal and a knowledge of relative liquid and gas densities. Finally, without changing the temperature at either the front or back of the cell, the laser was blocked and the polarization decay versus the time of the gas and liquid phases (starting from the saturation values) was recorded.

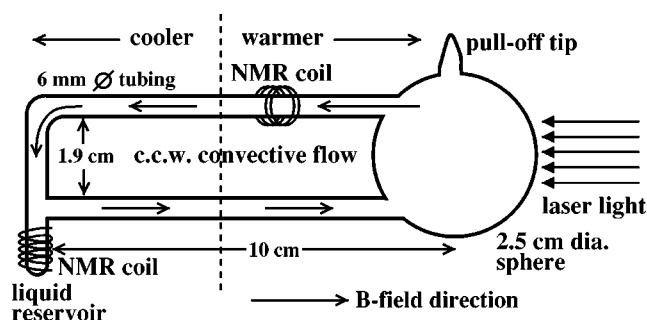


FIG. 1. Diagram of a xenon convection cell. The cell is permanently sealed at the pull-off tip and consists of one contiguous volume. Spin-exchange optical pumping of ^{129}Xe takes place in the front spherical chamber (where $T=360\text{--}380$ K), and convection transports the polarized gas to the liquid reservoir at the back of the cell (where $T=160\text{--}165$ K). Arrows indicate the direction of convective flow. The dashed line indicates the boundary between the hot and cold chambers in the oven/refrigerator.

TABLE I. Cells used in phase-exchange experiments. Shown for each cell are partial pressures of Xe, He, and N₂ (in mbar), maximum liquid P^ℓ and gas P^g polarizations, and the ratio N_ℓ/N_g of liquid to gas atoms.

Cell Name	Volume (cm ³)	P_{Xe}	P_{He}	P_{N_2}	N_ℓ/N_g	P_{max}^ℓ (%)	P_{max}^g (%)
45B	9.6	3750	670	67	3.2	6.3(0.7)	...
43B	9.4	3540	823	152	3.0	8.0(0.8)	...
43C	10.1	6520	0	69	6.3	5.0(0.5)	6.3(0.8)

We examined three different cells having xenon partial pressures between 3000 and 6500 mbar; the data are summarized in Table I. A maximum liquid polarization of 8% was achieved for the 3540 mbar cell. Example decay curves for the 6520 mbar cell are shown in Fig. 2. For the liquid signal it is apparent that a slower initial decay rate turned over at about $t=10$ min to a faster long-time rate.

We used MRI to provide a more quantitative estimate of the flow rate of gas around the convection loop and to assess the homogeneity of the liquid polarization during SEOP. Using the NMR coil on the top arm of the 3540 mbar cell, the magnetization in a 3-mm wide slice transverse to the flow direction was destroyed with a slice-selective rf pulse. The velocity of the gas was assessed by imaging the dark stripe at two known time points. The complex flow in the tube blurred the stripe rapidly, causing a large uncertainty in the velocity estimate, but we measured 18 ± 6 cm/s. The convective flow is counterclockwise with respect to the orientation shown in Fig. 1, as expected (gas falls on the cold side). We also acquired images of the liquid reservoir in the 6520 mbar cell at several time points after the laser was unblocked. We observed uniform signal intensity in the vertical direction and roughly parabolic intensity projections transverse to the cylinder axis, indicating uniform polarization. We attribute the uniformity to convection within the liquid, enhanced by brief intermittent boiling due to the temperature-control cycles.

We denote the numbers of Xe atoms in the gas and liquid phases by N_g and N_ℓ . The ratio $N_\ell/N_g = \sigma_g/\sigma_\ell$, where the right-hand side is the ratio of per-gas-atom to per-liquid-atom phase-exchange rates. The differential equations governing the evolution of the gas and liquid polarizations, P_{Xe}^g and P_{Xe}^ℓ , coupled by phase exchange, may then be written

$$\frac{dP_{\text{Xe}}^g}{dt} = (\overline{P_{\text{Rb}}} - P_{\text{Xe}}^g)\gamma_{\text{se}} - P_{\text{Xe}}^g\Gamma_g - (P_{\text{Xe}}^g - P_{\text{Xe}}^\ell)\sigma_g, \quad (1)$$

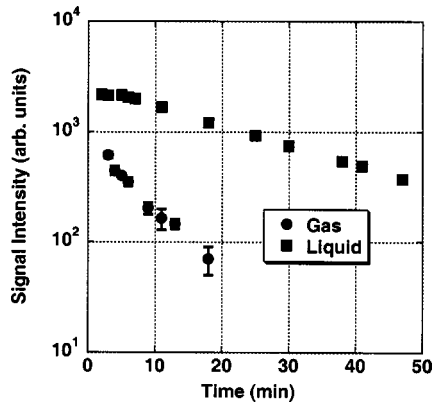


FIG. 2. Polarization-decay transients for liquid (squares) and gas (circles) in the 6520 mbar cell. The liquid decay more clearly shows evidence of biexponential behavior (see text); for times $t < 10$ min, the decay time is much longer than the later decay time of about 23 min.

$$\frac{dP_{\text{Xe}}^\ell}{dt} = -P_{\text{Xe}}^\ell\Gamma_\ell + (P_{\text{Xe}}^g - P_{\text{Xe}}^\ell)\sigma_\ell, \quad (2)$$

where $\overline{P_{\text{Rb}}}$ is the volume-averaged Rb polarization (assumed to be of order unity and time-independent), Γ_g is the volume-averaged gas-phase autorelaxation rate (dominated by wall relaxation), and Γ_ℓ is the liquid-phase autorelaxation rate. Our assumptions of uniform gas and liquid polarizations in the cell are reasonable in light of the large gas velocity and the uniformity of the liquid signal discussed above. (We note, however, that the cell may have critical “dead” areas of little or no convective flow.) At long times, Eqs. (1) and (2) become

$$P_{\text{Xe}}^g = \overline{P_{\text{Rb}}} \frac{\gamma_{\text{se}}}{\gamma_{\text{se}} + \Gamma_g + (\sigma_g\Gamma_\ell/\sigma_\ell + \Gamma_\ell)}, \quad (3)$$

$$P_{\text{Xe}}^\ell = \frac{\sigma_\ell P_{\text{Xe}}^g}{\Gamma_\ell + \sigma_\ell}. \quad (4)$$

Thus, the usual limitation on the final polarization P_{Xe}^g has an additional limiting term in the denominator that increases for larger values of N_ℓ/N_g , i.e., when the liquid-atom “load” being polarized by the gas atoms increases. We observe $P_{\text{Xe}}^\ell < P_{\text{Xe}}^g$, indicating that σ_ℓ is only several times faster than Γ_ℓ for our cells.

Equations (1) and (2) have a general solution that may be written

$$P_{\text{Xe}}^g = G_1 e^{-s_1 t} + G_2 e^{-s_2 t} + \phi, \quad (5)$$

$$P_{\text{Xe}}^\ell = \beta_1 G_1 e^{-s_1 t} + \beta_2 G_2 e^{-s_2 t} + \psi, \quad (6)$$

where the amplitude ratio G_2/G_1 and liquid-amplitude coefficients β_1 and β_2 are all determined by the various rates in the problem. The constants ϕ and ψ depend on the initial conditions of the experiment; they will both be zero for the case of the spin-down experiment (corresponding to $\overline{P_{\text{Rb}}}=0$). The theory thus predicts a biexponential behavior for the signal versus time for both the gas and liquid phases. The positive rate constants s_1 and s_2 are given by

$$s_{1,2} = \frac{1}{2}[(R_g + R_\ell) \pm \sqrt{(R_g - R_\ell)^2 + 4\sigma_g\sigma_\ell}], \quad (7)$$

where the total gas relaxation rate is $R_g = \gamma_{\text{se}} + \Gamma_g + \sigma_g$ and the total liquid relaxation rate is $R_\ell = \Gamma_\ell + \sigma_\ell$. For $N_\ell/N_g > 1$, it can be shown that $\beta_1 G_1 < 0$, while the other three amplitudes G_1 , G_2 , and $\beta_2 G_2$ are all positive.

For the rates and initial conditions (particularly $P_{\text{Xe}}^\ell < P_{\text{Xe}}^g$) involved here, the resulting liquid decay will start out slowly due to the negative coefficient $\beta_1 G_1$, and then at roughly $t=1/s_1$, the rate will increase asymptotically toward s_2 . Near $t=0$, phase exchange with the larger gas polarization causes the initial apparent slower decay of the liquid polarization. The gas-polarization decay has the same rate constants and two positive amplitudes, so it should start out with a faster relaxation rate and change over at around $t=1/s_1$ to the long-time rate s_2 . These qualitative behaviors were observed for both phases (Fig. 2). We have made theoretical estimates of s_1 and s_2 for the 6520 mbar cell using the following values based on the cell parameters and SEOP conditions: $\gamma_{\text{se}}^{-1} = 10$ min, $\Gamma_\ell^{-1} = 20$ min, $\Gamma_g^{-1} = 60$ min, $\sigma_\ell = 2.5\Gamma_\ell$, and $\sigma_g = 6.3\sigma_\ell$. The last two estimates are based on having initial gas and liquid polarizations of 6% and 5%, respec-

tively, and on $N_e/N_g=6.3$ for the 6520 mbar cell (see Table I). We calculate $s_1=1.9 \text{ min}^{-1}$ and $s_2=0.059 \text{ min}^{-1}$.

The calculated value for s_2 is in reasonable agreement with the data in Fig. 2, while s_1 estimated from the data is roughly an order of magnitude smaller than predicted. Uncertainty in the phase-exchange rates due to large relative uncertainties in the measured polarizations and our limited knowledge of the true flow dynamics may account at least in part for the discrepancy.

We envision at least two possible uses for liquid xenon polarized by SEOP and phase exchange. First, rapid volatilization of the liquid could provide a substantial quantity of highly polarized ^{129}Xe gas for various applications. It is not yet clear the degree to which our scheme could compete with "flow-through" xenon accumulator systems^{5,6} in producing large amounts of polarized ^{129}Xe . Our scheme has the advantage of avoiding the solid phase, whereby polarization losses in the freeze-thaw cycles are common.¹⁹ However, our production rate is ultimately limited by the 20 min relaxation time of liquid ^{129}Xe . Second, as a solvent, the liquid column would be a platform for polarization-transfer experiments,^{20–22} particularly since the ^{129}Xe polarization could be maintained at a steady-state value. Our cell design and implementation were an outgrowth of a previous experiment and are thus not well optimized. The gas polarization could be improved with a more powerful laser and by optimizing SEOP temperature, the optics train, and laser alignment. A faster phase-exchange rate could be achieved by eliminating dead volumes in the convection loop and maximizing the surface area of the liquid. In the limit of very fast phase-exchange rates, the biexponential behavior observed here should disappear.

We are grateful to M.S. Conradi and R.H. Price for helpful discussions. We thank J. Kyle and K. Teaford for assistance with cell fabrication. This work was supported by the National Science Foundation (PHY-0134980).

- ¹T. G. Walker and W. Happer, *Rev. Mod. Phys.* **69**, 629 (1997).
- ²A. Cherubini and A. Bifone, *Prog. Nucl. Magn. Reson. Spectrosc.* **42**, 1 (2003).
- ³M. P. Ledbetter and M. V. Romalis, *Phys. Rev. Lett.* **89**, 287601 (2002).
- ⁴B. M. Goodson, *J. Magn. Reson.* **155**, 157 (2002).
- ⁵B. Driehuys, G. D. Cates, E. Miron, K. Sauer, D. K. Walter, and W. Happer, *Appl. Phys. Lett.* **69**, 1668 (1996).
- ⁶A. L. Zook, B. B. Adhyaru, and C. R. Bowers, *J. Magn. Reson.* **159**, 175 (2002).
- ⁷I. A. Nelson and T. G. Walker, *Phys. Rev. A* **65**, 012712 (2002).
- ⁸C. H. Tseng, R. W. Mair, G. P. Wong, D. Williamson, D. G. Cory, and R. L. Walsworth, *Phys. Rev. E* **59**, 1785 (1999).
- ⁹R. W. Mair, C.-H. Tseng, G. P. Wong, D. G. Cory, and R. L. Walsworth, *Phys. Rev. E* **61**, 2741 (2000).
- ¹⁰M. A. Bouchiat, J. Brossel, and L. C. Pottier, *J. Chem. Phys.* **56**, 3703 (1972).
- ¹¹Pierce Biotechnology, Rockford, IL 61105.
- ¹²X. Zeng, E. Miron, W. A. van Wijngaarden, D. Schreiber, and W. Happer, *Phys. Lett.* **96A**, 191 (1983).
- ¹³B. Driehuys, G. D. Cates, and W. Happer, *Phys. Rev. Lett.* **74**, 4943 (1995).
- ¹⁴Spectra Gases, Alpha, NJ 08865.
- ¹⁵Tecmag, Inc., Houston, TX 77036.
- ¹⁶B. Chann, I. Nelson, and T. G. Walker, *Opt. Lett.* **25**, 1352 (2000).
- ¹⁷A. C.H. Hallett, in *Argon, Helium and the Rare Gases*, edited by G. A. Cook (Interscience, New York, 1961).
- ¹⁸B. Saam and M. S. Conradi, *J. Magn. Reson.* **134**, 67 (1998).
- ¹⁹N. N. Kuzma, B. Patton, K. Raman, and W. Happer, *Phys. Rev. Lett.* **88**, 147602 (2002).
- ²⁰J. C. Leawoods, B. Saam, M. S. Conradi, *Chem. Phys. Lett.* **327**, 359 (2000).
- ²¹R. J. Fitzgerald, K. L. Sauer, and W. Happer, *Chem. Phys. Lett.* **284**, 87 (1998).
- ²²G. Navon, Y.-Q. Song, T. Rööm, S. Appelt, R. E. Taylor, and A. Pines, *Science* **271**, 1848 (1996).